arXiv:hep-ph/9909524v1 28 Sep 1999

Resonances and higher twist in polarized lepton-nucleon scattering*

J. Edelmann, G. Piller, N. Kaiser and W. Weise

February 1, 2008

Physik-Department, Technische Universität München,
D-85747 Garching, Germany

Abstract

We present a detailed analysis of resonance contributions in the context of higher twist effects in the moments of the proton spin structure function g_1. For each of these moments, it is found that there exists a characteristic Q^2 region in which (perturbative) higher twist corrections coexist with (non-perturbative) resonance contribution of comparable magnitude.

PACS: 12.38.Cy, 13.60.Hb, 13.88.+e

*Work supported in part by DFG and BMBF

1 Introduction

High energy lepton scattering is a well established tool to investigate the structure of the nucleon. We restrict ourselves to charged leptons (e or μ); the exchanged virtual photon transfers four-momentum $q^\mu = (q_0, \boldsymbol{q})$, with the resolution determined by the virtuality $Q^2 = -q^2 = \boldsymbol{q}^2 - q_0^2$. At $Q^2 \gg 1\mathrm{GeV}^2$ deep-inelastic scattering resolves the partonic constituents (quarks and gluons) of the nucleon. At $Q^2 \lesssim 1\mathrm{GeV}^2$, on the other hand, the excitation of nucleon resonances and multi-pion continuum states is important. Exploring the transition between partonic and hadronic scales is of great significance to our understanding of the nucleon. The aim of the present paper is to discuss polarized lepton-nucleon scattering in kinematic regions where both hadron and parton degrees of freedom are expected to coexist.

The response of the nucleon is expressed in terms of the hadronic tensor

$$\begin{aligned} W_{\mu\nu}(x,Q^2) &= \frac{1}{4\pi}\sum_X (2\pi)^4\delta^4(P+q-P_X)\langle N(P,S)|J_\mu(0)|X(P_X,\lambda_X)\rangle \\ &\quad \langle X(P_X,\lambda_X)|J_\nu(0)|N(P,S)\rangle \\ &= W^{(S)}_{\mu\nu} + W^{(A)}_{\mu\nu}. \end{aligned} \tag{1}$$

The matrix elements of the electromagnetic current J_μ describe the transition of a nucleon with four-momentum P, invariant mass M ($P^2 = M^2$) and spin S to a hadronic final state X with four-momentum P_X and polarization λ_X. The sum in (1) implies an integration over three-momentum, $\frac{d^3P_X}{(2\pi)^3 2P_{X0}}$, and the normalization of $|N\rangle$ and $|X\rangle$ is $\langle N(P',S)|N(P,S)\rangle = 2P_0(2\pi)^3\delta^3(\boldsymbol{P'}-\boldsymbol{P})\delta_{S,S'}$.

The symmetric part $W^{(S)}_{\mu\nu}$ involves the spin independent structure functions $F_{1,2}$ measured in the scattering of unpolarized particles. The antisymmetric term,

$$W^{(A)}_{\mu\nu} = i\epsilon_{\mu\nu\lambda\sigma}q^\lambda\left[\frac{g_1(x,Q^2)}{P\cdot q}S^\sigma + \frac{g_2(x,Q^2)}{(P\cdot q)^2}(P\cdot q\, S^\sigma - q\cdot S\, P^\sigma)\right]. \tag{2}$$

introduces the spin structure functions g_1 and g_2. The nucleon spin vector is $S^\sigma = \frac{1}{2}\bar{u}(P,S)\gamma^\sigma\gamma_5 u(P,S)$ with Dirac spinors normalized as $\bar{u}u = 2M$. The structure functions depend on the Bjorken variable $x = Q^2/(2P\cdot q)$ and on Q^2.

Spin structure function data have been taken at SLAC, CERN and DESY [1, 2, 3, 4], primarily in the partonic high Q^2 range. Polarized deep-inelastic scattering in the resonance region was measured by the E143 collaboration at SLAC [1]. In the first part of our study we combine these data with other available information from the photo- and leptoproduction of nucleon resonances and investigate their contribution to the moments of the proton spin structure function g_1.

The influence of resonances and non-resonant low-mass excitations turns out to be quite significant for $Q^2 \lesssim 4$ GeV^2, as we shall demonstrate. For example, at $Q^2 = 2$ GeV^2

they account for as much as 20% of the first moment of g_1. Similar observations have been made for unpolarized deep-inelastic scattering [5].

In the second part we use the QCD operator product expansion and extract twist-4 matrix elements from the leading moments of g_1. For the first moment such an analysis has been carried out in great detail in ref.[6]. We find substantial higher-twist contributions to the first, third and fifth moments of g_1 for $Q^2 \lesssim 2, 4$ and 10 GeV^2, respectively. We examine target mass effects and investigate the different components of the higher-twist pieces of g_1. It turns out that contributions from elastic scattering, low-mass hadronic excitations and the partonic high-mass continuum are all of similar importance. We comment on the applicability of the twist expansion and recall basic ideas of parton-hadron duality. Altogether our results emphasize the need for high-precision experiments in the resonance region, to be performed at the Jefferson laboratory [7].

2 Twist expansion of g_1

In this section we briefly summarize results from the operator product expansion for the nucleon spin structure function g_1 (for details see e.g. [8]). Following the conventions of ref.[9] we introduce the n-th moment of g_1 as:

$$g_1^{(n)}(Q^2) = \int_0^1 \mathrm{d}x\, x^{n-1} g_1(x, Q^2) \qquad (\text{with} \quad \mathrm{n} = 1, 3, 5 \ldots). \tag{3}$$

Note that the upper limit of integration includes the contribution from elastic scattering. Its presence results from the fact that the operator product expansion, applied to deep-inelastic scattering, implicitly involves a sum over all final hadronic states including the nucleon itself. The importance of the elastic component in a QCD analysis of structure function moments has been emphasized in ref.[5].

At large momentum transfers, $Q^2 \gg \Lambda^2_{\mathrm{QCD}}$, the moments (3) can be written in terms of the twist expansion [10]:

$$g_1^{(n)}(Q^2) = \sum_{\tau=2,4,\ldots} \frac{\mu_\tau^{(n)}(Q^2)}{Q^{\tau-2}}. \tag{4}$$

"Twist" is a useful bookkeeping device to classify the light cone singularity of the coefficients in the QCD operator product expansion. Let a local operator in this expansion be a Lorentz tensor of rank r with (mass) dimension d, and let $\sigma \leq r$ be the "spin"associated with this operator. Then twist is defined as $\tau = d - \sigma$. The functions $\mu_\tau^{(n)}(Q^2)$ are related to nucleon matrix elements of quark and gluon operators with maximal twist τ. Their leading (logarithmic) Q^2-dependence can be calculated perturbatively as a series expansion in the strong coupling constant α_s. It should be mentioned that, due to the asymptotic nature of QCD perturbation theory, a systematic separation of the twist expansion and the perturbation series for $\mu_\tau^{(n)}$ is non-trivial and still a matter of ongoing investigations (for detailed discussions see e.g ref.[11]).

Up to corrections of order $1/Q^4$ one finds :

$$\begin{aligned} g_1^{(n)}(Q^2) &= \frac{1}{2}a_{n-1}(Q^2) + \frac{M^2}{Q^2}\frac{n(n+1)}{2(n+2)^2}\left(n\,a_{n+1}(Q^2) + 4\,d_{n+1}(Q^2)\right) \\ &+ \frac{4}{9}\frac{M^2}{Q^2}f_{n+1}(Q^2) + \mathcal{O}\left(\frac{M^4}{Q^4}\right) \end{aligned} \tag{5}$$

The coefficients a_n represent the genuine twist-2 contributions to $g_1^{(n)}$. They depend only logarithmically on Q^2 and dominate for Q^2 much larger than a typical hadronic scale, say the squared nucleon mass M^2. The second term in (5) arises from target mass corrections [12]. They are determined by the twist-2 pieces a_n and the twist-3 corrections d_n related to moments of the spin structure function g_2 [13] :

$$d_{n-1} = 2\,g_1^{(n)} + \frac{2n}{n-1}\,g_2^{(n)} + \mathcal{O}\left(\frac{M^4}{Q^4}\right). \tag{6}$$

The true twist-4 contributions in eq.(5) are denoted by f_{n+1}. For higher moments, $n > 1$, several matrix elements of twist-4 are involved. Their sum gives the coefficient f_{n+1} in (5).

In our work twist-2 contributions are defined through moments of presently available NLO parametrizations of g_1 [14]. The extraction of higher twist contributions from structure function data has been a subject of recent studies [6]. The active interest in these quantities derives from the fact that they are related to matrix elements which are sensitive to quark-gluon interactions in the nucleon. For example, one has [8, 15]:

$$2f_2(Q^2)M^2S^\mu = \sum_f e_f^2\langle N(P,S)|g\bar{\psi}_f\tilde{G}^{\mu\nu}\gamma_\nu\psi_f|N(P,S)\rangle. \tag{7}$$

The sum is taken over all quark fields ψ_f with flavor f and charge e_f, and $\tilde{G}^{\mu\nu}$ stands for the dual gluon field strength tensor (g denotes the QCD coupling strength).

3 Helicity amplitudes

In this paper we investigate contributions to the proton spin structure function g_1^p resulting from the electro-production of nucleon resonances, as well as from the production of continuum states in the deep-inelastic regime. Resonance contributions are conveniently described in terms of helicity amplitudes [16]:

$$G_m = \frac{1}{2M}\left\langle X(P_X, \lambda' = m - \frac{1}{2})\right|\epsilon^m \cdot J(0)\left|N(P, \lambda = -\frac{1}{2})\right\rangle. \tag{8}$$

We choose $\boldsymbol{q}/|\boldsymbol{q}|$ as the spin quantization axis. The amplitude G_m represents the production of a hadronic state X with spin projection λ' following the absorption of a virtual

photon with polarization (helicity) $m = \pm 1, 0$ on a nucleon with spin projection $\lambda = -1/2$. The photon polarization vectors are $\epsilon^{\pm} = (0, \mp 1, -i, 0)/\sqrt{2}$ and $\epsilon^0 = (|\boldsymbol{q}|, 0, 0, \nu)/Q$, with $Q = \sqrt{Q^2}$.

Combining eqs.(1) and (8) gives:

$$g_1 = \frac{1}{1 + \frac{Q^2}{\nu^2}} \sum_X M^2 \delta(W^2 - M_X^2) \left[|G_+|^2 - |G_-|^2 + \frac{\sqrt{2\,Q^2}}{\nu} G_0^* \, G_+ \right], \tag{9}$$

with $\nu = P \cdot q/M$. The final state X with invariant mass M_X has $\lambda' = +1/2$ for G_+, $\lambda' = -3/2$ for G_-, and $\lambda' = -1/2$ for G_0. It is common to use the amplitudes (e is the electric charge with $e^2/4\pi = 1/137$):

$$A_{1/2} = e \sqrt{\frac{M}{W^2 - M^2}} \, G_+, \quad A_{3/2} = e \sqrt{\frac{M}{W^2 - M^2}} \, G_-, \quad S_{1/2} = e \sqrt{\frac{M}{W^2 - M^2}} \frac{|\boldsymbol{q}^*|}{Q} \, G_0, \tag{10}$$

where $\boldsymbol{q}^*$ denotes the three-momentum transfer as measured in the photon nucleon center-of-mass frame, i.e. $\boldsymbol{q}^{*2} = Q^2 + (W^2 - M^2 - Q^2)^2/4W^2$ with the total c. m. energy W.

4 Model

In the following we present a parametrization of the proton structure function g_1^p which is applicable at small and moderate values of Q^2. We follow hereby closely an analysis of recent data in ref.[1]. At small center-of-mass energies, $W < 1.7$ GeV, we account for the contribution of dominant nucleon resonances. In addition, a phenomenological non-resonant background is added. For large $W > 1.7$ GeV we use an existing parametrization of available data.

The contribution of an isolated nucleon resonance to g_1 is usually expressed through helicity dependent virtual photon-nucleon cross sections. In terms of the helicity amplitudes (10) these are defined as:

$$\begin{aligned}
\sigma^T_{1/2,3/2} &= \frac{M\Gamma_R}{M_R[(W - M_R)^2 + \Gamma_R^2/4]} |A_{1/2,3/2}|^2, \\
\sigma^L_{1/2} &= \frac{M\Gamma_R}{M_R[(W - M_R)^2 + \Gamma_R^2/4]} \frac{Q^2}{\boldsymbol{q}^{*2}} |S_{1/2}|^2, \\
\sigma^{LT}_{1/2} &= \frac{M\Gamma_R}{\sqrt{2} M_R[(W - M_R)^2 + \Gamma_R^2/4]} \frac{Q}{|\boldsymbol{q}^*|} \, S^*_{1/2} A_{1/2}.
\end{aligned} \tag{11}$$

Here M_R is the mass and Γ_R the width of the resonance. Combining eqs.(9,10,11) gives for the contribution of a resonance R to g_1:

$$g_1(x, Q^2)\Big|_R \;=\; \frac{\nu M - Q^2/2}{4\pi^2 \alpha} \frac{1}{1 + Q^2/\nu^2} \left(\frac{\sigma^T_{1/2} - \sigma^T_{3/2}}{2} + \frac{Q}{\nu} \sigma^{LT}_{1/2} \right), \tag{12}$$

where the photon-nucleon cross sections refer to the excitation of R. At low W the helicity amplitudes are reasonably well known only for the photoproduction of the prominent nucleon resonances. In the case of electro-production accurate data are rare (for a review see e.g. [17]). We restrict ourselves to the dominant low mass resonances $\Delta(1232)$, $S_{11}(1535)$, and $D_{13}(1520)$. Our parametrizations of the corresponding helicity amplitudes are summarized in eqs.(13,14), with parameters given in Table 1.

At low center of mass energies the excitation of the $\Delta(1232)$ resonance is of particular importance. At small Q^2 it is dominated by a magnetic dipole transition which implies $A_{3/2}/A_{1/2} \approx \sqrt{3}$. Indeed, for real photons one finds $A_{3/2}/(\sqrt{3}A_{1/2}) \approx 1.064$ [18]. At large momentum transfers, $Q^2 \gg 1$ GeV^2, perturbative QCD gives $A_{3/2}/A_{1/2} \sim 1/Q^2$. However, it has been observed that even at $Q^2 = 3$ GeV^2 the magnetic dipole transition still dominates by far [19]. We can therefore assume $A_{3/2}/A_{1/2} \approx$ *const.* for $Q^2 \lesssim 3$ GeV^2. The Q^2-dependence of $A_{1/2}$ and $A_{3/2}$ is then extracted from an analysis of the Q^2-dependence of the transverse amplitude $|A_T|$ [17].

The S_{11} resonance has spin 1/2, so that the helicity amplitude $A_{3/2}$ is absent. We constrain the parametrization of the amplitude $A_{1/2}$ by the photo- and electro-production data from ref.[20].

For the $D_{13}(1520)$ the amplitude $A_{1/2}$ is found to be very small at $Q^2 = 0$. Here $A_{3/2}$ dominates. On the other hand data require $A_{1/2} > A_{3/2}$ for $Q^2 > 1$ GeV^2[17].

The parametrization in eqs.(13,14) agrees with the present, albeit quite rough, empirical information on the Q^2-dependence of the asymmetry $\mathcal{A}_1$ and the individual helicity amplitudes [17]:

$$|A_T| = \left(|A_{1/2}|^2 + |A_{3/2}|^2\right)^{1/2} = C\, \exp[-B\, Q^2], \tag{13}$$

and

$$|A_{1/2,3/2}| = \sqrt{\frac{1 \pm \mathcal{A}_1}{2}}\, |A_T|, \text{ with } \quad \mathcal{A}_1 = \frac{|\mathrm{A}_{1/2}|^2 - |\mathrm{A}_{3/2}|^2}{|\mathrm{A}_{1/2}|^2 + |\mathrm{A}_{3/2}|^2}, \tag{14}$$

with parameters given in table 1.

	$C/\mathrm{GeV}^{-1/2}$	B/GeV^{-2}	$\mathcal{A}_1$	Γ/GeV
$\Delta(1232)$	0.293	0.6	-0.545	0.12
$S_{11}(1535)$	0.07	0.17	1.0	0.15
$D_{13}(1520)$	0.16	0.83	$1 - \exp[0.3 - 1.5\, Q^2/\mathrm{GeV}^2]$	0.12

Table 1: Parameters for the helicity amplitudes in eqs.(13,14). The resonance widths Γ, which enter in eq.(11), are taken from ref.[18].

The interference term σ^{LT} involving the longitudinal and transverse photon-nucleon amplitudes is fairly unknown. Nevertheless, unpolarized scattering constrains the asymmetry

ratio:

$$\mathcal{A}_2 = \frac{2\sigma_{1/2}^{LT}}{\sigma_{1/2}^T + \sigma_{3/2}^T} < \sqrt{R(x,Q^2)}, \tag{15}$$

with $R = 2\sigma_{1/2}^L/(\sigma_{1/2}^T + \sigma_{3/2}^T)$. In the resonance region one finds on average $R = 0.06 \pm 0.02$ for $1\,\mathrm{GeV}^2 < \mathrm{Q}^2 < 8\,\mathrm{GeV}^2$ and $W < 1.7$ GeV [21]. Some fraction of this value is due to incoherent background contributions and not related to the excitation of single nucleon resonances. In the following we use $\mathcal{A}_2 = 0.08$. As a matter of fact, at $Q^2 > 1$ GeV^2, $\mathcal{A}_2$ contributes only very little to the structure function moments to be discussed later: changing $\mathcal{A}_2$ by 100% modifies our results for $g_1^{(1)}$ by less than 2%.

At low energies, $W < 1.7$ GeV, the structure function g_1 receives contributions also from non-resonant (multi-)meson production. However, hardly any empirical information is available here. We use a linear interpolation in the squared photon-nucleon center of mass energy W^2 which connects the inelastic threshold $W^2 = (M + m_\pi)^2$ with experimental data at $W > 1.7$ GeV.

Having modeled the structure function g_1^p at small center-of-mass energies, we continue to $W > 1.7$ GeV, where we use a parametrization from ref.[1] which reproduces data in the deep-inelastic region. This, finally, completes our model for g_1^p.

In Fig.1 we compare our model with recent g_1 data from the E143 collaboration taken at $Q^2 = 1.2$ GeV^2. Within the admittedly large experimental errors good agreement is found. A comparison of g_1^p, calculated with our model, and a parametrization of its deep-inelastic twist-2 part [14] is shown in Fig.2. At $Q^2 \lesssim 2$ GeV^2, significant deviations are apparent. The contributions of the S_{11} and D_{13} resonances are located around $x \sim 0.4$ at $Q^2 = 1$ GeV^2, while the excitation of the Δ occurs at $x \sim 0.6$. As Q^2 increases the low mass nucleon resonance excitations become less important. Furthermore, the contribution of nucleon resonances moves towards larger values of x, as one can see from the fact that the squared invariant mass of a particular nucleon excitation is fixed at $W^2 = M^2 + Q^2(1-x)/x$. Finally, at $Q^2 = 10$ GeV^2 our model coincides with the leading twist parametrization of ref.[14].

5 Analysis of moments of structure function

In this section we discuss the first moments of the proton structure function g_1 as obtained from the model previously described. In particular, we investigate the importance of contributions from elastic scattering, resonance production, target mass corrections, and true higher twist.

The elastic contribution, corresponding to the kinematic limit $x = 1$, is determined by

the Pauli and Dirac electromagnetic form factors of the nucleon as follows:

$$g_1^{(n)}(Q^2)\Big|_{el} = \frac{1}{2} F_1(Q^2) \left[F_1(Q^2) + F_2(Q^2) \right]. \tag{16}$$

In our numerical analysis we use parametrizations from ref.[22].

5.1 Resonance contributions

In order to investigate the role of low-mass nucleon excitations it is useful to introduce the ratio

$$\frac{g_1^{(n)}(Q^2)\Big|_{W_0}}{g_1^{(n)}(Q^2)} = \frac{\int_{x_0}^1 \mathrm{d}x x^{n-1} g_1(Q^2)}{\int_0^1 \mathrm{d}x x^{n-1} g_1(Q^2)}, \qquad \text{with } \; x_0 = x(W = W_0). \tag{17}$$

In the numerator we sum over all contributions of nucleon resonances and non-resonant multi-meson excitations with invariant mass $M_X < W_0 = 2$ GeV. In addition we always include the elastic part (16). Figure 3 shows that these low mass contributions to $g_1^{(n)}$ are quite sizable, especially for higher moments. For example, at $Q^2 = 2$ GeV^2 they are responsible for about 20% of the first moment $g_1^{(1)}$, while they account for 75% of $g_1^{(3)}$. With increasing n the role of low-mass excitations becomes evidently more pronounced. At the same time, the influence of the low-mass part of the spectrum also increases with decreasing Q^2. Roughly speaking, for $Q^2 < 2n$ GeV^2 low-mass excitations with $W < 2$ GeV account for more than 10% of $g_1^{(n)}$. At large Q^2 continuum contributions with $W > W_0$ take over. A similar observation has been made in an analysis of unpolarized lepton scattering [5].

5.2 Higher twist analysis

In order to extract the genuine higher twist coefficients f_n from the structure function moments $g_1^{(n)}$ one has to subtract twist-2 contributions and target mass corrections from each given moment. Returning to eq.(5) we have:

$$\begin{aligned} g_1^{(n)}(Q^2)|_{\mathrm{ht}} &= g_1^{(n)}(Q^2) - \frac{1}{2} a_{n-1}(Q^2) - \frac{M^2}{Q^2} \frac{n(n+1)}{2(n+2)^2} \Big(n\, a_{n+1}(Q^2) + 4\, d_{n+1}(Q^2) \Big) & (18) \\ &= f_{n+1} \frac{4}{9} \frac{M^2}{Q^2} + \mathcal{O}\left(\frac{M^4}{Q^4} \right). & (19) \end{aligned}$$

In the following we consider the first three moments, $n = 1, 3, 5$. We compare results obtained from our model for g_1^p with the twist-2 contributions $a_{n-1}/2$ from the NLO parametrization of ref.[14]. We also study the influence of target mass effects. Finally we discuss different contributions to the higher twist part $g_1^{(n)}(Q^2)|_{\mathrm{ht}}$.

In Fig.4 we compare the full moments $g_1^{(n)}$ with the leading twist parts, $a_{n-1}/2$, and the higher twist components $g_1^{(n)}(Q^2)|_{\rm ht}$. At small Q^2 one observes significant differences between $g_1^{(n)}$ and $a_{n-1}/2$. In particular one finds $g_1^{(n)}(Q^2)|_{\rm ht} > 0.1\, a_{n-1}/2$ for $Q^2 < 2$, 4, 10 GeV^2 and $n = 1$, 2, 3, respectively. The region where higher twist becomes important depends obviously on the moment n. For fixed Q^2 the difference between $g_1^{(n)}(Q^2)$ and $a_{n-1}/2$ increases with n. This is easily understood since contributions of low-mass nucleon excitations are enhanced in higher moments as pointed out in the previous section. Also shown in Fig.4 is the size of target mass effects. Since the coefficients d_n are not known accurately we use $d_n = 0$ which is compatible with present data [1, 2] and corresponds to the Wandzura-Wilczek conjecture [23]. For this choice target mass effects are indeed small. As an example, at $Q^2 = 2$ GeV^2 and n=1,3,5 they amount to less than 10% of the higher twist part. To estimate the uncertainty of this result we also use d_n obtained from eq.(6) for $g_2(x) = 0$. In this case target mass effects increase significantly and lead to a decrease of $g_1^{(n)}(Q^2)|_{\rm ht}$ by about 30%. High precision data on the spin structure function g_2, which are of course interesting in their own right, are therefore an important ingredient in the QCD analysis of g_1 itself.

Twist-4 contributions to $g_1^{(n)}$ are proportional to $1/Q^2$ (up to logarithmic corrections). In order to have a closer look at these terms it is instructive to plot the higher-twist moments $g_1^{(n)}(Q^2)|_{\rm ht}$ versus $1/Q^2$, as done in Fig. 5. Their approximately linear behavior indicates that twist-4 contributions play indeed a dominant role in $g_1^{(n)}(Q^2)|_{\rm ht}$. Neglecting terms of twist-6 and higher gives $f_2^p \simeq 0.1$ at $Q^2 = 2$ GeV^2, which agrees quite well with the analysis of ref.[6]. Further estimates can be found in ref.[15].

In the same figure we show the separate contributions to $g_1^{(n)}(Q^2)|_{\rm ht}$ from elastic scattering and from low-mass excitations with $(M + m_\pi) < W < 2$ GeV. Evidently, none of these contributions is small, in fact they all are of the same order of magnitude as $g_1^{(n)}(Q^2)|_{\rm ht}$ itself.

These observations emphasize the need for high-precision measurements especially in the resonance region. Upcoming data from TJNAF [7] are certainly welcome here. Figure 5 also points to the crucial role played by the elastic piece (16). Its proper treatment requires accurate information on the nucleon electromagnetic form factors in the range 1.5 GeV$^2 < Q^2 < 10$ GeV^2.

For the higher moments with $n = 3, 5$ the kinematic window in which twist-4 contributions dominate, that is, where $g_1^{(n)}(Q^2)|_{\rm ht}$ behaves linearly with $1/Q^2$, moves successively to higher Q^2. Again the contributions from elastic, resonant and non-resonant scattering all turn out to be of similar importance.

5.3 Parton-hadron duality

With decreasing Q^2 the higher twist contributions eventually reach the magnitude of the leading twist parts. As a consequence the twist expansion (4) breaks down. Our model for g_1^p can be used to suggest where this transition takes place: for a given moment $g_1^{(n)}$ higher twist contributions amount to less than 50% of the leading twist ones if $Q^2 > n$ GeV^2. On the other hand, we have learned in section 5.1 that low mass excitations account for more than 10% of $g_1^{(n)}$ if $Q^2 < 2n$ GeV^2.

This indicates a region of n and Q^2 in which perturbative higher twist corrections coexist with resonance contributions. The resonance terms are significant, and the transition amplitudes involving these resonances introduce powers of $1/Q^2$ in just such a way that they follow the deep-inelastic, large Q^2 behaviour of g_1^p.

Such a behavior is known as parton-hadron duality, a notion introduced by Bloom and Gilman for the unpolarized structure function F_2. A QCD explanation of this phenomenon has first been offered in ref.[24] and was further elaborated in ref.[25]. According to our results similar arguments apply to polarized lepton-nucleon scattering.

6 Summary

i) Contributions from the region of the nucleon resonances are an essential ingredient in the "higher-twist" analysis of the spin structure function g_1. Their effects are clearly visible in g_1^p even at Q^2 as large as 5 GeV^2. For example, low mass excitations with $W < 2$ GeV account for more than 50% of the 3rd moment and more than 80% of the 5th moment of g_1^p in the range $Q^2 \lesssim 3$ GeV^2.

ii) We have pointed to the importance of the elastic scattering ($x = 1$) part in a consistent moment analysis of g_1. Without inclusion of this elastic part, an extraction of higher-twist terms would not be meaningful.

iii) We observe a coexistence of resonance contributions and perturbative higher-twist corrections in a window, roughly framed by n GeV^2 $< Q^2 <$ $2n$ GeV^2, where $n = 1, 3, 5, \ldots$ denotes the moment of g_1. The understanding of this coexistence region in terms of parton-hadron duality is an interesting issue. Precision data from TJNAF will help clarifying these questions in the near future.

Acknowledgments:

The authors wish to acknowledge helpful discussions with K.A. Griffioen and L. Mankiewicz.

References

[1] E143, K. Abe *et al.* Phys. Rev. **D58** (1998) 112003
E143, K. Abe *et al.* Phys. Rev. Lett. **76** (1996) 587

[2] E154, K. Abe et al., Phys. Lett.**B404** (1997) 377
E154, K. Abe et al., Phys. Lett. **B405** (1997) 180
E154, K. Abe et al., Phys. Rev. Lett. **79** (1997) 26
E155, P.L. Anthony et al., (1999), hep-ex/9904002
E155, P.L. Anthony et al., (1999), hep-ex/9901006

[3] SMC, B. Adeva et al., Phys. Rev. **D58** (1998) 112001
SMC, B. Adeva et al., Phys. Rev. **D58** (1998) 112002

[4] HERMES, A. Airapetian et al., Phys. Lett. **B442** (1998) 484
HERMES, K. Ackerstaff et al., Phys. Lett. **B404** (1997) 383

[5] X. Ji and P. Unrau, Phys. Rev. **D52** (1995) 72

[6] X. Ji and W. Melnitchouk, Phys. Rev. **D56** (1997) 1

[7] V. Burkert, D. Crabb and R. Minehart Exp.91-023

[8] E.V. Shuryak and A.I. Vainshtein, Nucl. Phys. **B199** (1982) 451 E.V. Shuryak and A.I. Vainshtein, Nucl. Phys. **B201** (1982) 141

[9] B. Ehrnsperger, A. Schafer and L. Mankiewicz, Phys. Lett. **B323** (1994) 439

[10] X. Ji and P. Unrau, Phys. Lett. **B333** (1994) 228

[11] A.H. Mueller, Phys. Lett. **B308** (1993) 355

[12] A. Piccione and G. Ridolfi, Nucl. Phys. **B513** (1998) 301

[13] R.L. Jaffe and X. Ji, Phys. Rev. **D43** (1991) 724

[14] T. Gehrmann and W.J. Stirling, Phys. Rev. **D53** (1996) 6100

[15] E. Stein, P. Górnicki, L. Mankiewicz, A. Schäfer, Phys. Lett. **B353** (1995) 107
B. Ehrnsperger and A. Schafer, Phys. Rev. **D52** (1995) 2709
G.G. Ross and R.G. Roberts, Phys. Lett. **B322** (1994) 425
I.I. Balitsky, V.M. Braun and A.V. Kolesnichenko, Phys. Lett. **B242** (1990) 245 Erratum Phys. Lett. **B318**(1993) 648
J. Balla, M.V. Polyakov and C. Weiss, Nucl. Phys. **B510** (1998) 327

[16] C.E. Carlson and N.C. Mukhopadhyay, Phys. Rev. **D58** (1998) 094029.

[17] P. Stoler, Phys. Rept. **226** (1993) 103

V.Burkert in G.A. Miller, Seattle, USA, July 1-12, 1991," *Singapore, Singapore: World Scientific (1992) 244 p. (The national Institute for Nuclear Theory series).*

V.Burkert, Czechoslovak Journal of Physics Vol bf 46 (1996) No 7/8

[18] C. Caso *et al.*, Eur. Phys. J. **C3** (1998) 1

[19] V.D. Burkert, Phys. Rev. Lett. **75** (1995) 3614

[20] H. Breuker *et al.*, Zeit. Phys. **C13** (1982) 113

H. Breuker *et al.*, Z. Phys. **C17** (1983) 121

E. Evangelides *et al.*, Nucl. Phys. **B71** (1974) 381

F.W. Brasse, W. Flauger, J. Gayler, S.P. Goel, R. Haidan, M. Merkwitz and H. Wriedt, Nucl. Phys. **B110** (1976) 413

F.W. Brasse *et al.*, Nucl. Phys. **B139** (1978) 37

[21] C. Keppel, Ph.D. Thesis, American University, 1994

[22] P. Mergell, U.G. Meissner and D. Drechsel, Nucl. Phys. **A596** (1996) 367

[23] S. Wandzura and F. Wilczek, Phys. Lett. **72B** (1977) 195

[24] H. Georgi and H.D. Politzer, Phys. Rev. **D14** (1976) 1829

[25] A. De Rujula, H. Georgi and H.D. Politzer, Ann. Phys. **103** (1977) 315

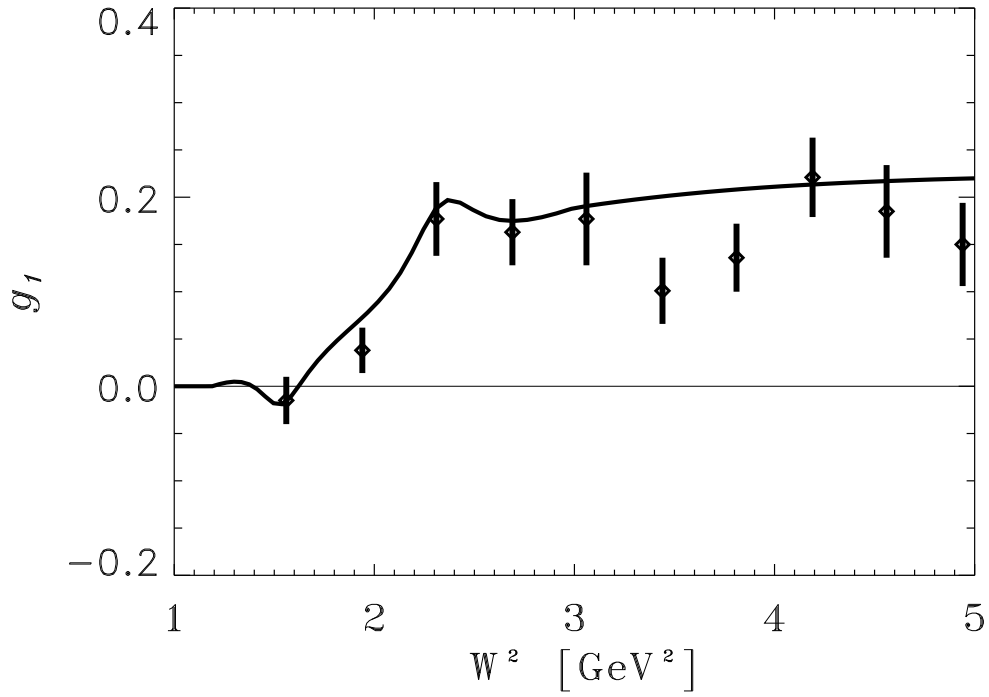

Figure 1: The proton spin structure function g_1^p at $Q^2 = 1.2$ GeV^2 as calculated from our model in section 4. The data are taken from ref.[1].

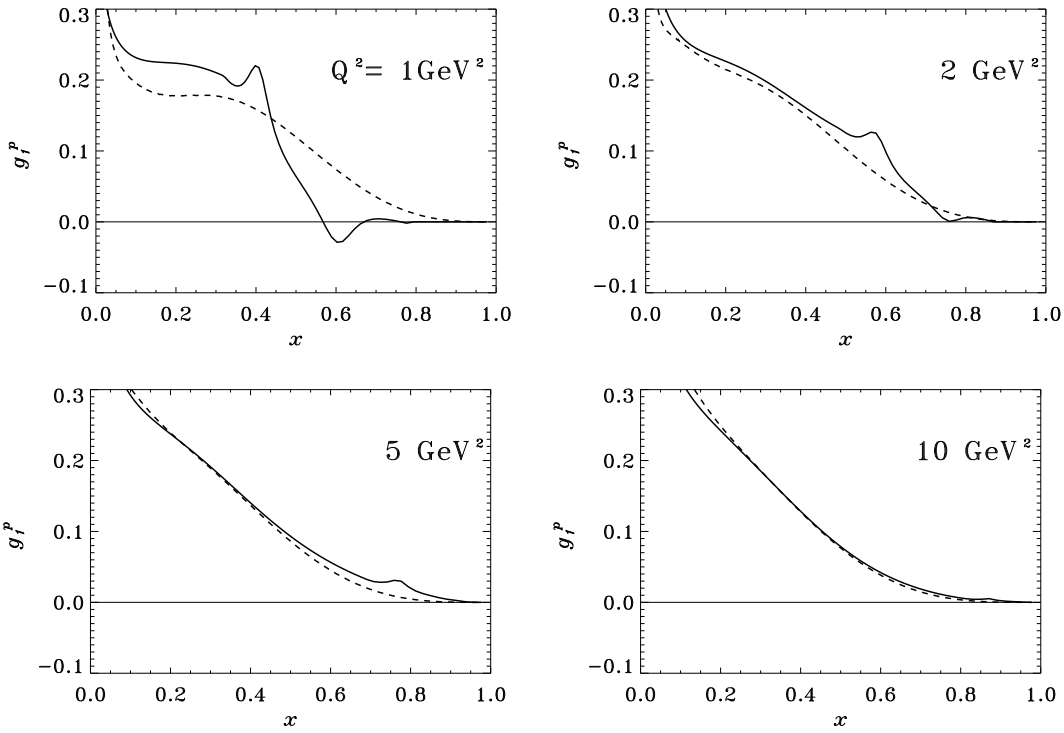

Figure 2: The x-dependence of g_1^p for $Q^2 = 1, 2, 5$ and 10 GeV^2. The full lines show results of the model developed in section 4, the dashed lines correspond to the twist-2 parametrization of ref.[14]

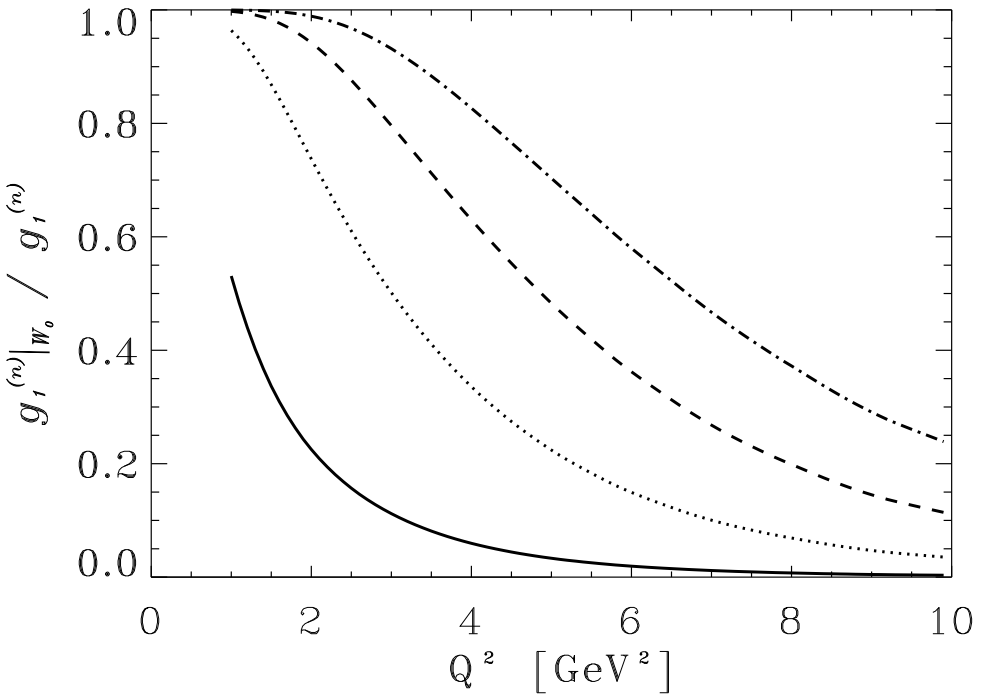

Figure 3: Contribution to the moments $g_1^{(n)}$ from low mass excitations with $W < W_0 = 2$ GeV, normalized to the full moments. Shown are the 1$^{\rm st}$ (full), 3$^{\rm rd}$ (dotted), 5$^{\rm th}$ (dashed), and 7$^{\rm th}$ (dash-dotted) moments.

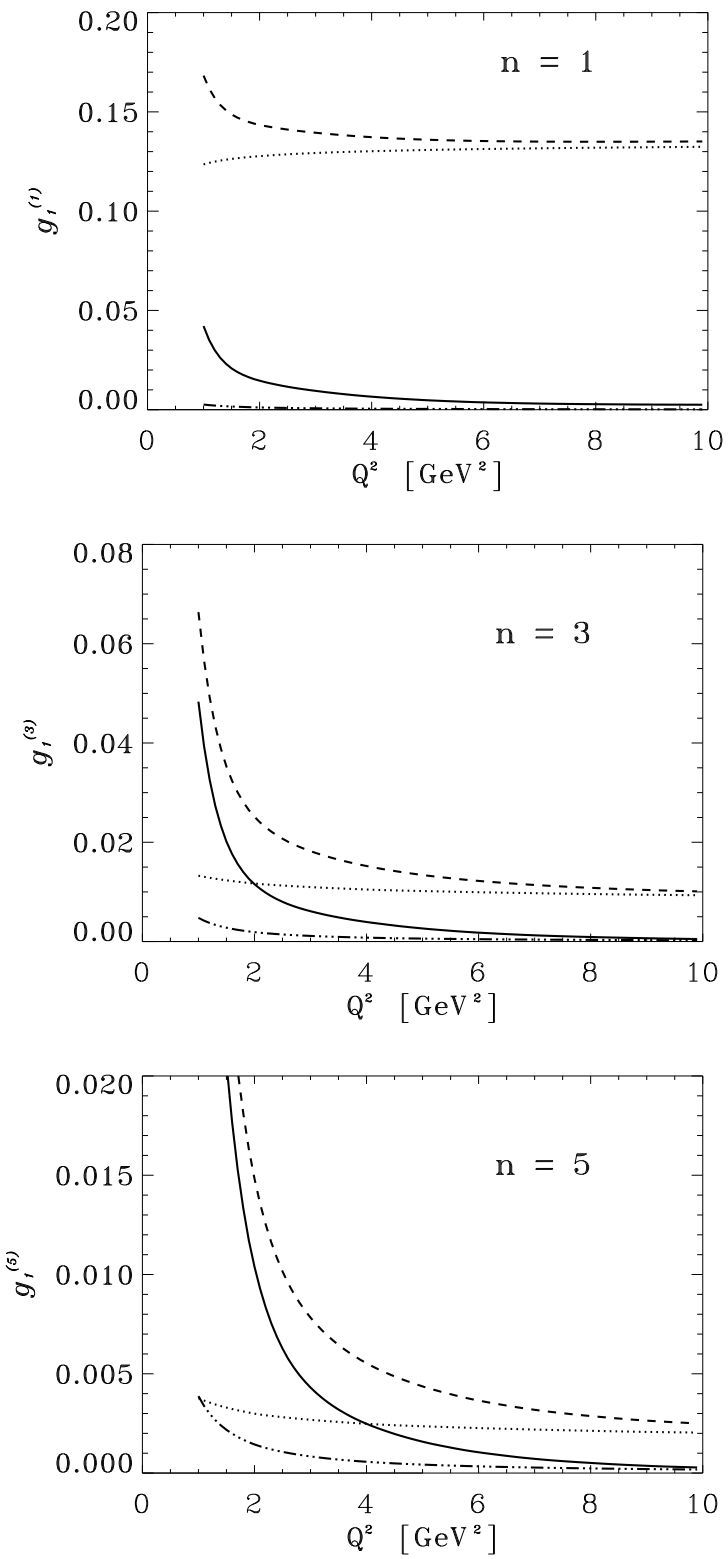

Figure 4: The moments $g_1^{(n)}$ and their decomposition (18) for $n = 1, 3$ and 5. Shown are: $g_1^{(n)}$ (dashed), the twist-2 part $a_{n-1}/2$ (dotted), the target mass corrections (dash-dotted), and the higher twist piece $g_1^{(n)}|_{\rm ht}$ of Eq.(18) (full).

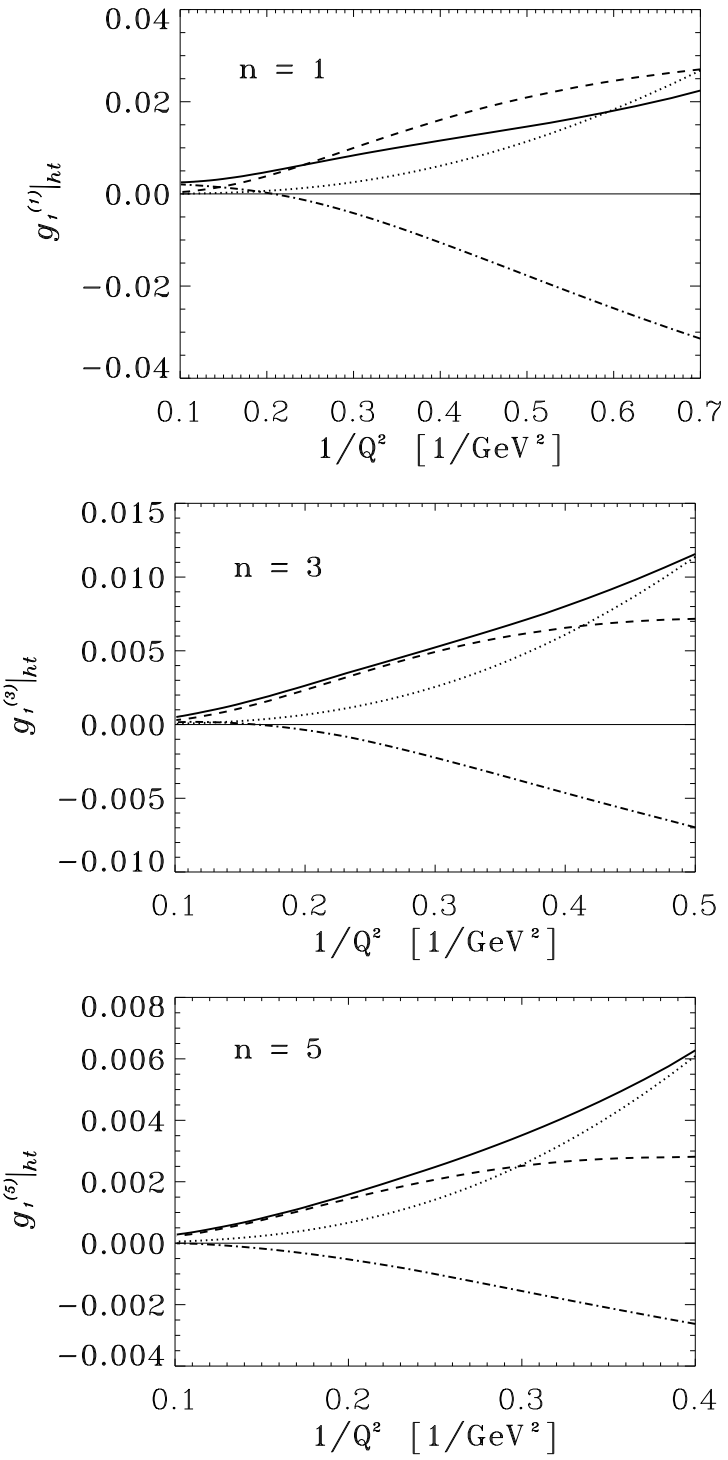

Figure 5: Higher twist components $g_1^{(n)}|_{\rm ht}$ for $n = 1, 3$ and 5 and their decomposition, plotted as a function of $1/Q^2$. Shown are $g_1^{(n)}|_{\rm ht}$ (full), the elastic part (dotted), contributions from low-mass excitations with $W < W_0 = 2$ GeV (dashed), and the difference between the high-mass continuum with $W > W_0$ and the twist-2 part (dash-dotted).